Femtosecond pulse shaping using the geometric phase

Bilal Gökce,[1] Yanming Li,[2] Michael J. Escuti,[2] and Kenan Gundogdu[1,*]

[1]*Physics Department, NC State University, 2401 Stinson Dr., Raleigh, North Carolina 27695, USA*

[2]*Electrical and Computer Engineering, NC State University, 2410 Campus Shore Dr., Raleigh, North Carolina 27695, USA*

**Corresponding author: kenan_gundogdu@ncsu.edu*

Received December 16, 2013; revised February 5, 2014; accepted February 5, 2014;
posted February 10, 2014 (Doc. ID 201301); published March 12, 2014

We demonstrate a femtosecond pulse shaper that utilizes polarization gratings to manipulate the geometric phase of an optical pulse. This unique approach enables circular polarization-dependent shaping of femtosecond pulses. As a result, it is possible to create coherent pulse pairs with orthogonal polarizations in a 4f pulse shaper setup, something until now that, to our knowledge, was only achieved via much more complex configurations. This approach could be used to greatly simplify and enhance the functionality of multidimensional spectroscopy and coherent control experiments, in which multiple coherent pulses are used to manipulate quantum states in materials of interest. © 2014 Optical Society of America

OCIS codes: (320.5540) Pulse shaping; (350.1370) Berry's phase; (120.6200) Spectrometers and spectroscopic instrumentation; (240.5440) Polarization-selective devices.

http://dx.doi.org/10.1364/OL.39.001521

Femtosecond pulse shaping is a powerful technique to tailor ultrashort optical pulses into desired temporal and spectral forms [1]. Most commonly, a 4f configuration with an electrically controllable element, such as an acousto-optic modulator (AOM) [2,3] or a spatial light modulator (SLM) [4,5], is positioned at the Fourier plane, which shapes the pulses by manipulating the phase of the optical fields in their frequency domain. In this traditional approach, the phase control is achieved through an optical path length difference effect, fundamentally related to the wave's velocity, manipulating the dynamic phase [6,7]. A single optical pulse could be converted into almost arbitrarily complicated waveforms of multiple pulses with precise time separations, amplitudes, spectra, and pulse widths without sacrificing the coherence [8]. This may be used in many complex experiments, including coherent control of electronic or vibrational excitations to manipulate a chemical reaction [9–12], tracing electronic coherences in multidimensional experiments [13–15], and/or coherent control of dark and bright states in atomic and more complex quantum systems [16,17].

Optical pulses are defined by how their amplitude, phase, and polarization vary in time (and frequency), and all three parameters influence light-matter interactions. While the manipulation of amplitude and phase is relatively straightforward using prior methods, the control of pulse polarization has been much more challenging. For instance, a single SLM-based 4f configuration can implement a spatially varying optical path length to introduce phase differences among spectral components in the Fourier domain [4]. However, its output always has the same polarization as the input. In the only known approach achieving full control of optical pulse amplitude, phase, and polarization, Weise and co-workers developed a complex design involving three SLMs, half-wave plates, and polarizers in the Fourier plane [18,19].

Control of pulse polarization in a pulse shaper setup is useful in many applications. For instance, in multidimensional spectroscopy, pulse shaping is commonly used to create two time-delayed pulses to excite the sample. This simple application of pulse shaping greatly simplifies the experiment, because these two pulses are inherently phase stable [13]. However it limits the pulses to the same polarization state. Excitation with orthogonal polarizations greatly enhances the capability of the multidimensional experiments as it enables easier extraction of cross peaks, and study of coherent excitation dynamics involving differently oriented transition dipoles [20]. The primary difficulties in femtosecond pulse polarization control are the inherent slowness of traditional switchable polarization optics and the fact that these are entirely distinct from the traditional (dynamic) phase controlling elements. In our approach, we sidestep these limitations via the Pancharatnam–Berry phase [21] (one type of geometric phase [6,22]) effect, a phenomenon where orthogonal polarizations traversing a birefringent layer can take on equal and opposite amounts of phase delay (in addition to whatever change of polarization may occur). Thereby, we can achieve at least all the same phase manipulation effects in the Fourier plane of a pulse shaper but via a completely different phase (i.e., with the geometric, rather than, dynamic phase).

In this work, we demonstrate a femtosecond pulse shaper utilizing a polarization grating (PG), illustrated in Fig. 1. This element is formed with anisotropic materials in such a way as to spatially manipulate the geometric phase, [23–25] but not the dynamic phase (i.e., in contrast to AOMs and SLMs). Physically, a PG [26,27] is a birefringent thin-film with half-wave retardation thickness, with an optical axis that varies spatially as $\Phi(x) = \pi x/\Lambda$, where Λ is the grating pitch. Optically, there are two equally valid ways of considering a PG. From one perspective, a PG provides a purely linear phase shift, analogous to a prism and without 2π resets, which is equal to $2\pi x/\Lambda$. From another perspective, a PG is a periodic grating structure with 100% diffraction into its first orders. Either way, the linear phase sweep across the spectra in the Fourier domain results in a uniform time delay of an optical pulse. For our pulse shaper, the transfer function of the PG is as follows (adapted from [28,29]):

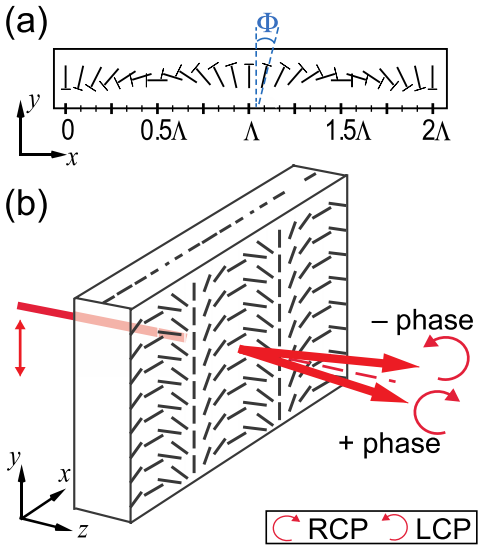

Fig. 1. PG structure, with an in-plane optical axis (small lines) profile whose orientation angle varies linearly. (a) Plan view. (b) Perspective view, showing linearly p-polarized input transferred into two parts: RCP with positive phase change and LCP with negative phase change.

$$E_{\text{in}}e^{-i\phi}|\text{in}\rangle \overset{PG}{\rightarrow} |\langle \text{RCP}|\text{in}\rangle|E_{\text{in}}e^{-i(\phi-2\Phi(x))}|\text{LCP}\rangle + |\langle \text{LCP}|\text{in}\rangle|E_{\text{in}}e^{-i(\phi+2\Phi(x))}|\text{RCP}\rangle, \quad (1)$$

where $|\text{in}\rangle$ denotes the input polarization, and $|\text{RCP}\rangle$ and $|\text{LCP}\rangle$ denote right and left circular polarization, respectively.

Note that $\pm 2\Phi(x,y) = \pm 2\pi x/\Lambda$ is the net phase change (via Pancharatnam–Berry effect) caused by the PG, for the LCP and RCP components [two output terms in Eq. (1)], respectively. Input polarization determines the LCP/RCP ratio and further determines the weighting between these two waves. A special case of linearly polarized input is shown in Fig. 1(b), with both phase modulations of equal power. Therefore, when a PG with pitch Λ is placed at the Fourier plane of the pulse shaper, a linear phase per unit length of $\pm 2\pi/\Lambda$ will be applied to the frequency components and result in shifted pulse(s) in the time domain. The amount of this shift is simply related to and controllable by the PG pitch. More interestingly, the shift can happen in both forward and backward directions using the same PG, by adjusting the input polarization.

The polymer PGs in this work were fabricated using photo-alignment of polymerizable liquid crystal materials, of the same kind described in [30,31]. It is designed to have a first-order efficiency of >99% in the range 780–830 nm, with a peak at ~806 nm.

Figure 2 illustrates the standard 4f pulse shaper and the cross-correlation setup for measuring the shaped pulses. 140 fs pulses centered at 806 nm with a bandwidth of 20 nm are generated by a Ti:sapphire oscillator (Mira 900, Coherent). The first diffraction grating (1200 g/mm) disperses p-polarized pulses. A 200 mm focal length cylindrical lens focuses each spectral component horizontally on the PG located at the Fourier plane. A second identical cylindrical lens and grating combination brings the

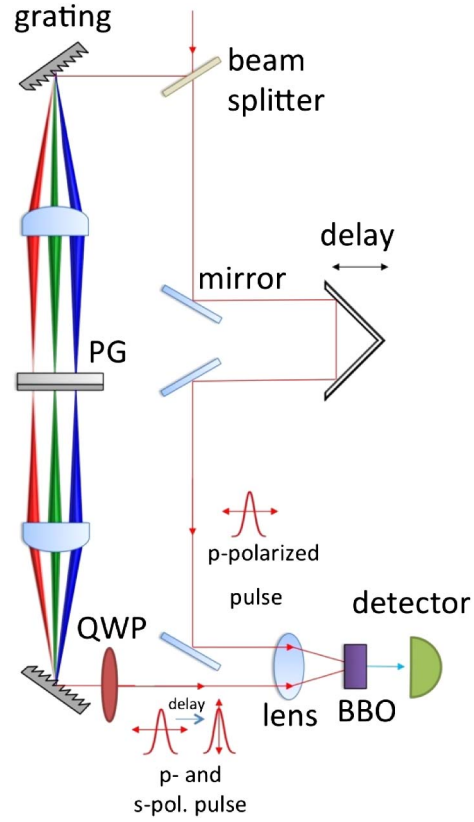

Fig. 2. Experimental setup of PG-based pulse shaper. Femtosecond p-polarized pulses are chromatically dispersed and focused onto a PG positioned at the Fourier plane. The output is collected and combined with a time-delayed reference pulse for analysis by a BBO crystal and photodetector.

spectral components back into the time domain. The outputs are time separated LCP and RCP pulses. A zero-order quartz quarter-wave plate (QWP) positioned after the second grating transforms RCP and LCP into p- and s-polarized light, respectively. The output pulses are mixed with a reference pulse in a BBO crystal for cross-correlation. Type-I phase matching only allows p-polarization to interact with the BBO. Delay of the reference pulse is controlled with a translation stage.

The throughput of the second diffraction grating (identical to the first) is not polarization independent (i.e., its transmittance is 36% and 64% for p- and s-polarization, respectively). Therefore the incident RCP and LCP pulses are elliptically polarized after the second grating. We estimate the degree of ellipticity after the second grating as 0.73, which is easily corrected by a 4.5° offset of the QWP.

Figure 3 shows the result for the time delayed oppositely polarized pulses. At 0°, the QWP creates ±45° linearly polarized pulses with the +45° polarized pulse delayed to −0.5 ps and the −45° polarized pulse delayed to +0.5 ps. At −40.5° of the QWP the first pulse is s-polarized whereas the second pulse is p-polarized; hence we only observe the sum-frequency generation (SFG) in the BBO due to the first not the second pulse.

Because of the periodic nature of the PG structure, there is a small diffraction angle (0.033°) between the LCP and RCP pulses. As we intended, the time-separated output pulses are parallel to each other but have an 11 μm

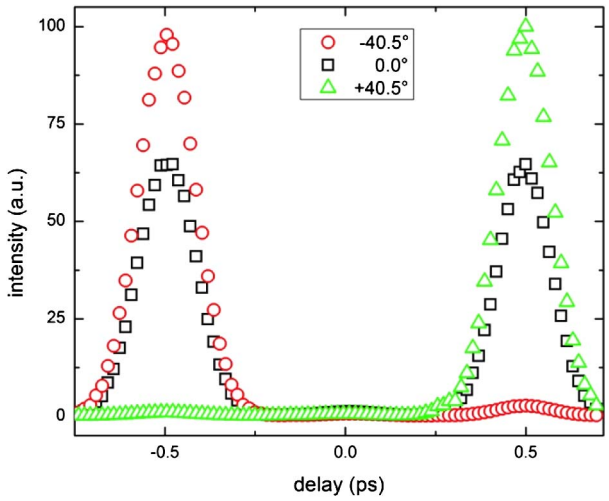

Fig. 3. Cross-correlation of shaped pulses measured by SFG with a reference pulse in a BBO crystal. Type I phase matching only allows *p*-polarization to mix with the reference pulse. By setting the QWP to ±40.5° the two orthogonally polarized pulses at delays −0.5 ps (circles) and 0.5 ps (triangles) are measured. At 0° QWP setting both pulses partially mix with *p*-polarized reference pulse (squares).

spatial separation. Shorter focal length lenses in the pulse shaper could minimize this separation.

Figure 4 shows the results of pulse shaping with PGs with different grating periods Λ to demonstrate the variability of the time delay for LCP pulses. The PGs used in these measurements are static, and the time delay between pulses can only be adjusted by manually replacement of PG elements. Note, however, that it is straightforward to employ electrically switchable PG stacks [32–35], similar to prior work on nonmechanical beam steering [36,37]. This would enable these selectable linear phase functions, in order to enable active control of the delay in a similar fashion compared to the equivalent SLM system, but with additional capability of creating coherent orthogonally polarized pulses.

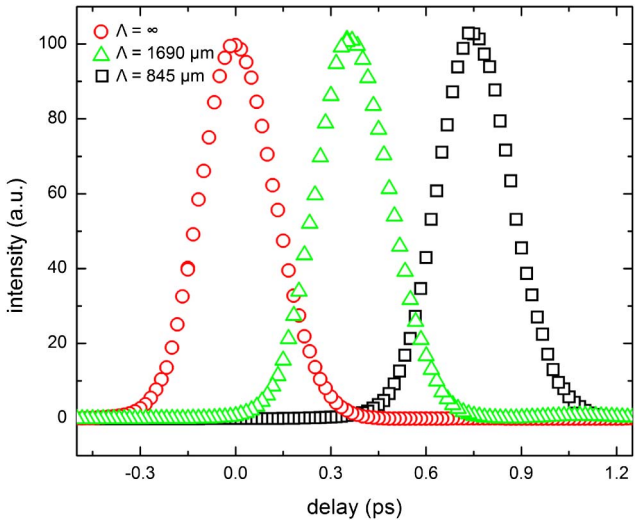

Fig. 4. Delay of LCP pulses using PGs with different grating periods. The PG with Λ = ∞ is a half-wave plate that introduces same phase for all frequencies. Hence it does not result in a delay.

It is important to note that in the current demonstration, we only implemented linear phase functions in the Fourier plane. Thus the design is limited to create time delays that are polarization dependent. However by using geometric phase elements with nonlinear phase functions [28,29], more complex waveforms could be achieved.

In conclusion, we demonstrate 4f pulse shaping using PGs, which manipulate the geometric phase of an optical pulse. Unlike the traditional approaches using SLMs or holographic gratings formed in isotropic materials, our method directly couples to the polarization state of the pulse. This achieves the same phase manipulation effects in the Fourier plane of a pulse shaper as the traditional dynamic phase approach, but instead via the geometric phase. This enables additional functionality because multiple pulses with orthogonal polarizations can be produced. The pulse shaper described here is static, i.e., the time delay can only be changed by manually installing a different PG. However, by using multiple stacks and electrically addressable liquid crystals, it should be possible to electrically adjust the delays between the pulses. Looking ahead, such capability will make possible nearly any set of multiple phase-coherent pulses with tailored time separations and spectral profiles for many challenging applications including multidimensional spectroscopy and coherent control experiments.

MJE and YL gratefully acknowledge the support of the National Science Foundation (NSF grant ECCS-0955127).

References

1. A. M. Weiner, Opt. Commun. **284**, 3669 (2011).
2. M. A. Dugan, J. X. Tull, and W. S. Warren, J. Opt. Soc. Am. B **14**, 2348 (1997).
3. M. Roth, M. Mehendale, A. Bartelt, and H. Rabitz, Appl. Phys. B **80**, 441 (2005).
4. A. M. Weiner, Rev. Sci. Instrum. **71**, 1929 (2000).
5. J. C. Vaughan, T. Hornung, T. Feurer, and K. A. Nelson, Opt. Lett. **30**, 323 (2005).
6. M. Martinelli and P. Vavassori, Opt. Commun. **80**, 166 (1990).
7. P. F. McManamon, P. J. Bos, M. J. Escuti, J. Heikenfeld, S. Serati, H. Xie, and E. A. Watson, Proc. IEEE **97**, 1078 (2009).
8. A. Monmayrant, S. Weber, and B. Chatel, J. Phys. B **43**, 103001 (2010).
9. D. Goswami, Phys. Rep. **374**, 385 (2003).
10. K. Ohmori, Annu. Rev. Phys. Chem. **60**, 487 (2009).
11. M. Dantus and V. V. Lozovoy, Chem. Rev. **104**, 1813 (2004).
12. A. Assion, T. Baumert, M. Bergt, T. Brixner, B. Kiefer, V. Syfried, M. Strehle, and G. Gerber, Science **282**, 919 (1998).
13. S. H. Shim and M. T. Zanni, Phys. Chem. Chem. Phys. **11**, 748 (2009).
14. K. Gundogdu, K. W. Stone, D. B. Turner, and K. A. Nelson, Chem. Phys. **341**, 89 (2007).
15. K. W. Stone, K. Gundogdu, D. B. Turner, X. Q. Li, S. T. Cundiff, and K. A. Nelson, Science **324**, 1169 (2009).
16. D. Meshulach and Y. Silberberg, Nature **396**, 239 (1998).
17. S. Chen, A. Jaron-Becker, and A. Becker, Phys. Rev. A **82**, 013414 (2010).
18. F. Weise and A. Lindinger, Opt. Lett. **34**, 1258 (2009).
19. M. Plewicki, F. Weise, S. M. Weber, and A. Lindinger, Appl. Opt. **45**, 8354 (2006).
20. C. T. Middleton, D. B. Strasfeld, and M. T. Zanni, Opt. Express **17**, 14526 (2009).
21. M. Berry, J. Mod. Opt. **34**, 1401 (1987).
22. S. Tiwari, J. Mod. Opt. **39**, 1097 (1992).

23. T. Todorov, L. Nikolova, and N. Tomova, Appl. Opt. **23**, 4588 (1984).
24. C. Oh and M. J. Escuti, Phys. Rev. A **76**, 043815 (2007).
25. M. V. Berry, J. Mod. Opt. **34**, 1401 (1987).
26. L. Nikolova and T. Todorov, J. Mod. Opt. **31**, 579 (1984).
27. J. Tervo and J. Turunen, Opt. Lett. **25**, 785 (2000).
28. E. Hasman, Z. Bomzon, A. Niv, G. Biener, and V. Kleiner, Opt. Commun. **209**, 45 (2002).
29. Y. Li, J. Kim, and M. J. Escuti, Appl. Opt. **51**, 8236 (2012).
30. G. P. Crawford, J. N. Eakin, M. D. Radcliffe, A. Callan-Jones, and R. A. Pelcovits, J. Appl. Phys. **98**, 123102 (2005).
31. M. J. Escuti, C. Oh, C. Sanchez, C. W. M. Bastiaansen, and D. J. Broer, Proc. SPIE **6302**, 630207 (2006).
32. R. K. Komanduri, W. M. Jones, C. Oh, and M. J. Escuti, J. Soc. Inf. Disp. **15**, 589 (2007).
33. R. K. Komanduri and M. J. Escuti, Appl. Phys. Lett. **95**, 091106 (2009).
34. C. Provenzano, P. Pagliusi, and G. Cipparrone, Appl. Phys. Lett. **89**, 121105 (2006).
35. S. R. Nersisyan, N. V. Tabiryan, D. M. Steeves, and B. R. Kimball, J. Nonlinear Opt. Phys. Mater. **18**, 1 (2009).
36. J. Kim, C. Oh, S. Serati, and M. J. Escuti, Appl. Opt. **50**, 2636 (2011).
37. J. Kim, M. N. Miskiewicz, S. Serati, and M. J. Escuti, Proc. SPIE **8052**, 80520T (2011).